ISSN 2689-8268 | Volume 5

American Journal of Surgery and Clinical Case Reports

Case Report Open Access

Evaluation of Microtox and *Daphnia Magna* Acute Toxicity Assays after the Removal of Microorganisms and Organic Compounds from a Pharmaceutical Wastewater using Silver-Loaded Magnetic Nanoparticles

Öztekin R and Sponza DT*

Department of Environmental Engineering, Engineering Faculty, Dokuz Eylül University, Turkey

***Corresponding author:**

Delia Teresa Sponza,
Dokuz Eylül University, Engineering Faculty,
Environmental Engineering Department, Buca,
İzmir-Turkey, Tel: +90 232 412 11 79,
E-mail: delya.sponza@deu.edu.tr

Received: 10 Jul 2022
Accepted: 29 Jul 2022
Published: 04 Aug 2022
J Short Name: AJSCCR

Keywords:

Acute toxicity test; Aliivibrio fischeri (Vibrio fischeri); Daphnia magna; Field emission scanning electron microscope (FESEM); Fourier transform infrared spectrophotometer (FTIR); Ibuprophene; Microtox acute toxicity test; Oxytetracycline; pharmaceutical wastewater; silver loaded-magnetic nanoparticles (Ag-Fe_3O_4 NPs); X-ray diffraction (XRD) analysis; thermogravimetric analysis (TGA).

Citation:

Sponza DT. Evaluation of Microtox and Daphnia Magna Acute Toxicity Assays after the Removal of Microorganisms and Organic Compounds from a Pharmaceutical Wastewater using Silver-Loaded Magnetic Nanoparticles. Ame J Surg Clin Case Rep. 2022; 5(5): 1-12

1. Abstract

1.1. Background: In this study, silver-loaded magnetic nanoparticles (Ag-Fe_3O_4 NPs) were developed under laboratory conditions to treat the secondary settling effluent coming from the biological aerobic activated sludge proses from a Pharmaceutical Wastewater (ww).

1.2. Material and Methods: This wastewater contained some pharmaceuticals and bacteria at high concentrations which were not treated at the beginning treatment steps. The effect of Ag-Fe_3O_4 NPs concentrations (0.1, 0.5, 1.0, 1.5 mg/l), contacting time (2, 5, 8, 10 and 15 mins), pH levels (4, 7 and 8), power (2, 4 and 6 W/m^2), frequency (2, 5, 8 kHz). *Salmonella, Psuedomonas*, yeast, fungi, total coliforms, fecal coliforms, heterotrophic bacteria and ibuprophene, oxytetracycline removal yields were detected. The Ag-Fe_3O_4 NPs has a size of 25 nm and the saturation magnetization was recorded as 49 emu/g. The particle shapes and properties were analised with field emission scanning electron microscope (FESEM) and fourier transform infrared spectrophotometer (FTIR), X-ray diffraction (XRD) and thermogravimetric *analysis (*TGA). The acute toxicity assays was examined with Microtox (with *Aliivibrio fischeri* also known as *Vibrio fischeri*) and *Daphnia magna* acute toxicity test before and after the removal of microorganisms and organic compounds from a Pharmaceutical ww using Ag-Fe_3O_4 NPs. ANOVA statistical analysis was used for all experimental samples. A cost analysis also was performed.

1.3. Results: The maximum organism and pollutant yields were around 98% at 0.5 mg/l, after 10 mins at a neutral pH. The recovery of the Ag-Fe_3O_4 NPs were studied. 89% treatment yields were recorded after 8 months of continous operation. Adsorptive and photocatalytic studies showed that after a short adsortion time the pollutants and the microorganisms were removed successfully at 2 watt/m^2 power and at 2 kHz frequency. The proposes a novel simple method was applied for the adsorption of ibuprophene and oxytetracycline in water using Ag-Fe_3O_4 NPs. The TEM image of Ag-Fe_3O_4 NPs appeared darker than Fe_3O_4 NPs. Our method of NPs synthesis could not produce uniform particles in size. The XRD patterns of Ag-Fe_3O_4 NPs showed the 2θ values of 38.11°, 44.32°, 64.24°, 77.61° and 81.57° corresponding to the (111), (200), (220), (311) and (222) planes of cubic Ag, respectively. The Ms values was 61 emu/g for Fe_3O_4 NPs and 69 emu/g for Ag-Fe_3O_4 NPs. The increasing Ms values in the nanocomposites (NCs) might have been due to the interactions between the NPs changed the anisotropic energy. 99% maximum ibuprophene adsorption removal yield was obtained at 2.03 mg/g maximum ibuprophene adsorption concentration, at pH = 7.0 and at 21°C, respectively. 99% maximum oxytetracycline adsorption removal yield was observed at 3.04 mg/g maximum oxytetracycine adsorption concentration, at pH = 5.0 and at 21°C, respectively. 93% maximum Ag-Fe_3O_4

NPs adsorption yield was measured at 45 min contact time, 7 mg in 500 µl of suspension, at 0.1 mg/l Ag-Fe_3O_4 NPs, at 3.0 mg/l ibuprophene and at 3.0 mg/l oxytetracycline, respectively. 94.44% maximum Microtox acute toxicity yield was observed in Ag-Fe_3O_4 NPs=1 g/l after 150 min, at 60ºC. However, 90% maximum *Daphnia magna* acute toxicity yield was observed in Ag-Fe_3O_4 NPs=1 g/l after 150 min, at 60ºC. The removal of microorganisms and organic compounds from a Pharmaceutical ww using Ag-Fe_3O_4 NPs is a very economical method during different experimental conditions.

1.4. Conclusions: The characterization of the adsorbent by means of microscopy, spectroscopy and calorimetry techniques reveal the presence of Ag in Ag-Fe_3O_4 NPs and the adsorption of ibuprophene and oxytetracycline in Pharmaceutical ww. The adsorption equilibrium is characterized by a Langmuir isotherm model. Microtox acute toxicity test yield is higher than *Daphnia magna* acute toxicity test for the removal of microorganisms and organic compounds from Pharmaceutical ww using Ag-Fe_3O_4 NPs. Therefore, it can be concluded that the toxicity originating from the Ag-Fe_3O_4 NPs is not significant and the real acute toxicity throughout the removal of microorganisms and organic compounds was attributed to the Pharmaceutical ww, to the microorganisms and organic compounds in Pharmaceutical ww ww, to their metabolites and to the disruption by-products. Finaly, the removal of microorganisms and organic compounds from a Pharmaceutical ww using Ag-Fe_3O_4 NPs and the evaluation of Microtox and *Daphnia Magna* acute toxicity assays for these conditions was successfully implemented. The removal of microorganisms and organic compounds from a Pharmaceutical ww using Ag-Fe_3O_4 NPs is a very economical method during different experimental conditions.

2. Introduction

Pharmaceuticals are products used in large doses in daily life considered as contaminants of emerging concern. Due to the large amounts of drugs consumed, the hydrogenic sources sufer from contamination processes that give rise to toxicological efects in humans despite its low concentrations [1, 2]. Many medicines considered as emerging contaminants are constantly detected in groundwater, wastewater treatment plants and water supply. The inefciency of conventional methods used in water treatment plants to remove the contaminant motivates the development of efective methods to treat efuent contamination [3]. According to the physico-chemical properties of drugs, their degradation products and the characteristics of the soils, these substances can reach the groundwater and contaminate the aquifers or remain retained in the soil, thus afecting the ecosystem and humans through the food chain [4]. Additionally, the portion of medicines not assimilated by the organism, as well as chemical substances administered to animals, usually become part of wastewater. Consequently, diferent ways of removing medicines in waters have been studied [5].

In recent decades, much attention has been paid to the application of NPs in environmental purposes. This is because nanosized materials have a large surface area-to-mass ratio and high reactivity [6, 7]. Thanks to these features, NPs have been widely used as catalysts [8], adsorbents [9, 10], detectors [11], and disinfectants [12] in various studies. Due to their non-specific action, NPs as adsorbents are capable of removing a wide variety of contaminants including organics, inorganics, and colloids such as bacterial cells. When making a decrease in microbial contamination is a major goal, one can use some NPs with inherent disinfection capabilities such as magnetic NPs [13]. Therefore, the need for adding other disinfectants such as chlorine (Cl^{-1}) and ozone (O_3), which are associated with adverse side effects, may be eliminated [14].

Magnetite (Fe_3O_4) is the strongest magnetic species among the transient metal oxides [15]. The reactive surface of iron-oxides allows for the adsorption of various impurities from water environment [16]. When used as NPs, called Fe_3O_4 NPs, they release reactive oxygen species (ROS) such as superoxide radicals (O_2^-), hydroxyl radicals ($OH^•$), hydrogen peroxide (H_2O_2), and singlet oxygen ($^1O_2$) that can decompose proteins and DNA in bacterial cells [17]. Therefore, Fe_3O_4 NPs can exert their antibacterial effects through both physical adsorption and chemical disinfection. The feature of Fe_3O_4 NPs gives them an excellent separation property in the vicinity of an external magnetic field, which is essential for the removal of small-sized NPs from the effluent [14].

The federal government has developed regulations and guidelines to protect people from the possible health effects from long-term exposure to Ag in drinking water [18]. The Environmental Protection Agency (EPA) suggests that the level of Ag in drinking water not be more than 0.05 mg/l. However, in May, 1989, the EPA announced that this restriction on Ag levels in drinking water might be removed. For shortterm exposures (l-10 days), EPA suggests that drinking water levels of Ag not be more than 1.142 mg/l. Any release to the environment of more than 453.6 g silver nitrate ($AgNO_3$) or 453.6 kg of Ag alone should be reported to the National Response Center. To limit the amount Ag workers are exposed to during an 8-hour shift for a 40-hour work week, the Occupational Safety and Health Administration (OSHA) has set a legal limit (Permissible Exposure Limit or PEL) of 0.01 mg Ag/m^3 air in workroom air Studies in rats show that drinking water containing very large amounts of Ag (2.6 g Ag/l) is likely to be life-threatening [18].

World Health Organization (WHO) (2002) found that in environments not anthropogenically altered, silver sulfhydrate (AgHS) or simple sulfur (S) polymer species (HS-Ag-S-Ag-SH) dominate [19]. At higher concentrations, colloidal silver sulfide (Ag_2S) or silver polysulfide complexes dominate. Under reducing conditions, the Ag ion is sometimes released from the sulfur (S_8) bearing species. Because concentrations of the Ag ion is typically extremely low in natural environments relative to the available binding sites of S_8, the Ag ions are quickly combined with other S_8 comp-

lexes. Both scenarios result in essentially non-toxic forms of Ag. Hardness is also a significant control on Ag toxicity. However, it is not the largest control on toxicity as once thought. Below are the data used to create the Environmental Protection Agency (EPA) Ag toxicity equation as a function of hardness, re-evaluated by Hogstrand (1996) [19].

Ag is a noble metal that exhibits a relatively weak oxidation behavior [20]. In large sizes, it is a low-reactive metal. However, in nanoscales, its microbicidal characteristic extremely enhances due to the increased specific surface area [21]. Like Fe_3O_4 NPs, Ag NPs can exhibit their antibacterial activity through ROS generation [22]. In addition, other mechanisms have been mentioned such as the interaction of Ag-NPs with surface structures of bacterial cells and the reaction of released Ag ions with S_8 and phosphorous (P) of cell macromolecules [23]. Accordingly, Ag has been used successfully in previous studies as a bactericidal agent against Gram-negative bacteria, e.g., coliforms [24]. The easy separation of the Fe_3O_4 product can facilitate the recovery of invaluable Ag particles. It has been stated that Ag in combination with Fe_3O_4 NPs can penetrate biofilms more easily than Ag alone does [21]. Therefore, Fe_3O_4-Ag NPs can show enhanced characteristics for water and wastewater treatment purposes [14].

There are several assumptions for the interaction of Ag and Fe_3O_4 NPs. Petrov et al. [25] modified Fe_3O_4 NPs with Ag and could detect Ag both around Fe_3O_4 NPs and as separate particles in the structure of Ag-Fe_3O_4 NPs. They also showed that Ag ions replaced Fe^{+3} ions in the Fe_3O_4 lattice. Therefore, a combination of physical and chemical interactions can play a role in the connection of Ag to Fe_3O_4 NPs structure [14].

Various studies in the literature investigated the antibacterial effects of magnetic Fe_3O_4 NPs alone or in combination with Ag-NPs as shells. For example, Ghaseminezhad et al. [23] took advantage of the anti-biofilm activity of the compounds against antibiotic-resistant bacterial species in vitro. Joshi et al. [26] employed the composite successfully against *Escherichia coli (E. Coli)* using the zone inhibition method on culture plates. However, limited studies are available to compare the effectiveness of Fe_3O_4 NPs and Ag-Fe_3O_4 NPs against bacterial cells in environmental applications. Moreover, the efficacy of the NCs in the decrease of organic content of environmental samples would be interesting to determine. As far as we know, there is no similar study in the literature to investigate the application of Fe_3O_4 NPs and Ag-Fe_3O_4 NPs for advanced purification and disinfection of Wastewater Treatment Plant (WWTP) effluents.

This study aimed to examine the effectiveness of Fe_3O_4 NPs and Ag-Fe_3O_4 NPs in the removal of Total Coliforms (TC), Fecal Coliforms (FC), Heterotrophic Bacteria (HB), and Chemical Oxygen Demand (COD) from real Pharmaceutical WWTP effluents. In addition to, the particle shapes and properties were analised with Field Emission Scanning Electron Microscope (FESEM) and fourier transform infrared spectrophotometer (FTIR), X-ray Diffraction (XRD) and Thermogravimetric *Analysis (*TGA). The acute toxicity assays was examined with Microtox (with Aliivibrio *fischeri* also known as *Vibrio fischeri*) and *Daphnia magna* acute toxicity test before and after the removal of microorganisms and organic compounds from Pharmaceutical ww using Ag-Fe_3O_4 NPs. ANOVA Statistical Analysis was used for all experimental samples. A cost analysis also was performed.

3. Materials and Methods

3.1. Preparation of Ag-Fe_3O_4 NPs

20 ml of H_2O was heated at 80^{o}C and continuously stirred under N_2(g) atmosphere. Then, 0.56 g $FeCl_3.6H_2O$ and 0.2 g $FeCl_2.4H_2O$ were added. When the solids were dissolved, 2 ml of concentrated ammonia (NH_3) solution were incorporated and the solution was stirred for 10 min. The particles were separated using a permanent magnet and the supernatant was discarded. The solid was washed three times with H_2O until the washing liquids were neutral. 0.28 g Fe_3O_4 NPs were suspended in 20 ml of H_2O. After, 5.7 ml of diluted 0.011 g/l $AgNO_3$ solution were added, the mixture was stirred for 5 min and using the magnet were separated and washed several time with H_2O. Finally, Ag-Fe_3O_4 NPs were suspended in 20 ml of H_2O again.

3.2. Physicochemical Properties of Ag-Fe_3O_4 NPs

A Field Emission Scanning Electron Microscopy (FESEM) analysis was performed to check the presence of Ag in the samples. In Figure 1a it is shown the 3D image for Fe_3O_4, while Figure 1b shows the intensity image for Ag-Fe_3O_4 NPs where the Ag appears as spherical, and shiny due to its high atomic number.

Additionally, energy dispersive X-ray Spectroscopy (EDX) graphs for Ag-Fe_3O_4 NPs are presented in Figure 2. In the latter, the signal corresponding to Ag appears in the plot. A BET test was carried out to determine the contact surface area of the adsorbent, giving a value equal to 116.476 m^2/g, and a correlation coefficient for the BET isotherm of 0.999.

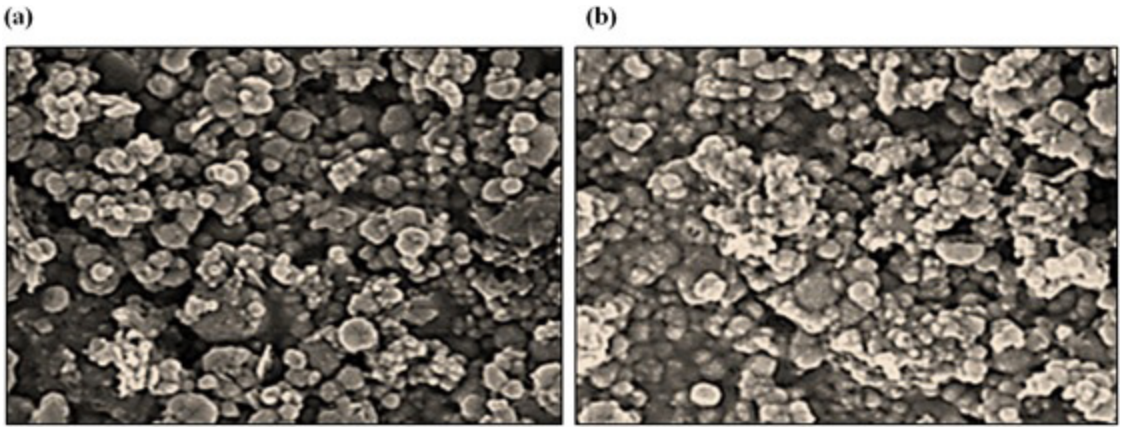

Figure 1: FESEM images of (a) Fe_3O_4 NPs and (b) Ag-Fe_3O_4 NPs

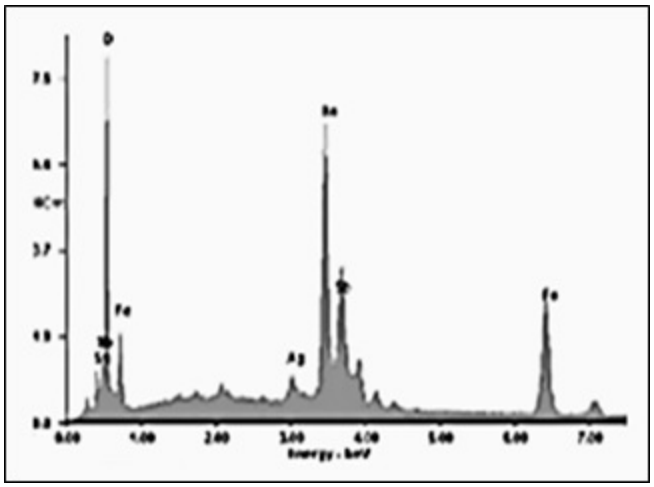

Figure 2: EDX spectra of Ag-Fe_3O_4 NPs

3.3. Adsorption Studies

A H_2O sample (10 ml) containing pharmaceuticals at concentrations of 0.2 mg/l was placed in a polypropylene tube, 500 µl of Ag-Fe_3O_4 NPs suspension were added. After shaking 30 min at 21°C, the magnet was placed at the bottom of the tube for 5 min and the adsorbent was separated. The supernatant was analyzed for ibuprophene ana oxytetracycline to determine the maximum removal efciency of the aforementioned chemicals. Figure 3 showed FTIR spectrum for Ag-Fe_3O_4 NPs after the adsorption process, where the characteristic IB signals are marked (carbonyl group at 1704,12 1/cm stretch frequencies of Csp3-H of isobutyl group at 2951,93 and 2922,15 1/cm; aromatic C=C bond at 1560,83 1/cm; O–H bond at 3100 1/cm).

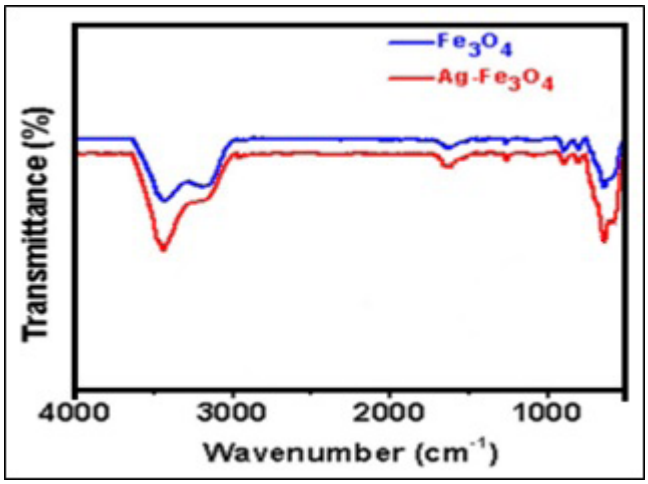

Figure 3: FTIR spectra of Fe_3O_4 NPs (blue) and Ag-Fe_3O_4 NPs (red)

3.4. Acute Toxicity Assays

3.4.1. Microtox Acute Toxicity Test

Toxicity to the bioluminescent organism *Aliivibrio* fischeri (also called *Vibrio fischeri* or *V. fischeri*) was assayed using the Microtox measuring system according to DIN 38412L34, L341, (EPS 1/RM/24 1992). Microtox testing was performed according to the standard procedure recommended by the manufacturer [27]. A specific strain of the marine bacterium, *V. fischeri*-Microtox LCK 491 kit [28] was used for the Microtox acute toxicity assay. Dr. LANGE LUMIX-mini type luminometer was used for the microtox toxicity assay [29].

3.4.2. *Daphnia magna* Acute Toxicity Test

To test toxicity, 24-h born *Daphnia magna* (*D. Magna*) were used as described in Standard Methods section 8711 A, B, C, D, E [30]. After preparing the test solution, experiments were carried out using 5 or 10 *Daphnia magna* introduced into the test vessels. These vessels had 100 ml of effective volume at 7.00– 8.00 pH, providing a minimum DO concentration of 6 mg/l at an ambient temperature of 20–25°C. Young *Daphnia magna* were used in the test (≤24 h old); 24–48 h exposure is generally accepted as standard for a *Daphnia magna* acute toxicity test. The results were expressed as mortality percentage of the *Daphnia magna*. Immobile animals were reported as dead *Daphnia magna*.

3.5 Statistical Analysis

Multiple regression analysis between y and x variables was performed using the Excell in Windows. The linear correlation was assessed with R^2. The significance of the correlations between data was determined using the ANOVA Test Statistics [31].

All experiments were carried out three times and the results given as the means of triplicate samplings.

4. Results and Discussions

4.1. NPs Characteristics

4.1.1. TEM Analysis Results

TEM images were recorded to examine the morphologies of Fe_3O_4 NPs and Ag-Fe_3O_4 NPs and determine the particle sizes. TEM images are presented in Figure 4. As can be observed, Fe_3O_4 NPs (Figure 4a) and Ag-Fe_3O_4 NPs (Figure 4b) were almost semi-spherical in shape. The TEM image of Ag-Fe_3O_4 NPs appeared darker than that of Fe_3O_4 NPs. It is also shown that our method of NPs synthesis could not produce uniform particles in size.

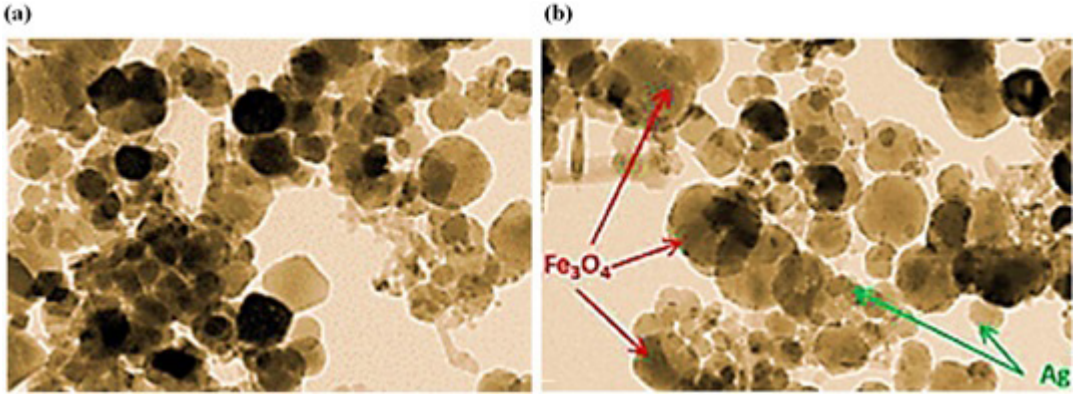

Figure 4: TEM images of **(a)** Fe_3O_4 NPs and **(b)** Ag-Fe_3O_4 NPs

The size of Fe_3O_4 NPs is dependent on various factors including synthesis conditions (e.g. oxygen-free environment) [32], pH of the synthesis medium [33], the ratio of base to iron (Fe) ions, and the length of the alkyl chain, respectively [34]. The mean diameter of particles in our study was 41 and 34 nm for Fe_3O_4 NPs and Ag-Fe_3O_4 NPs, respectively. The reduced size of particles by adding decorating agents has been also observed in the study by Joshi et al. [26]. They used the same method of NPs synthesis as in our study and reported a reduced diameter from 26 to 20 nm after decorating Fe_3O_4 NPs with Ag. It seems that a decrease in the amount of iron-oxide precursor per unit volume of the preparation solution might be a reason for the reduced particle size in Ag-Fe_3O_4 NPs. However, there are reports in the literature [35] showing that the diameter of NPs increases when Ag shells decorated Fe_3O_4 cores. The procedure of NPs synthesis has a major contribution to the characteristics of the NCs including the particle size. The particle sizes measured in this study conform to the findings of Naqvi et al. [36] study, reporting the mean size of superparamagnetic iron oxide NPs as 30 nm, and the findings of Ebrahimi et al. [37] study, producing Ag-Fe_3O_4 NPs in the range of 23 to 54 nm. The latter study showed that the particle size is dependent on reducing agents used in the synthesis process. Santoyo Salazar et al. [38] conducted a study on Fe_3O_4 NPs in the range of 10–40 nm and showed that NPs of smaller than 20 nm had poor Fe_3O_4 properties.

4.1.2. XRD Analysis Results

The results of XRD analysis of asprepared NCs (Figure 5). The characterization peaks were observed at 2θ values of 30.12°, 35.51°, 43.15°, 53.23°, 56.82°, and 62.34°, implying pure Fe_3O_4 in the Fe_3O_4 NPs structure. These values are in complete agreement with the values reported by Ebrahimi et al. [37] and attribute to the indices (220), (311), (400), (422), (511), and (440) for Fe_3O_4 arises, respectively. The XRD patterns of Ag-Fe_3O_4 NPs showed the 2θ values of 38.11°, 44.32°, 64.24°, 77.61° and 81.57° corresponding to the (111), (200), (220), (311), and (222) planes of cubic Ag, respectively.

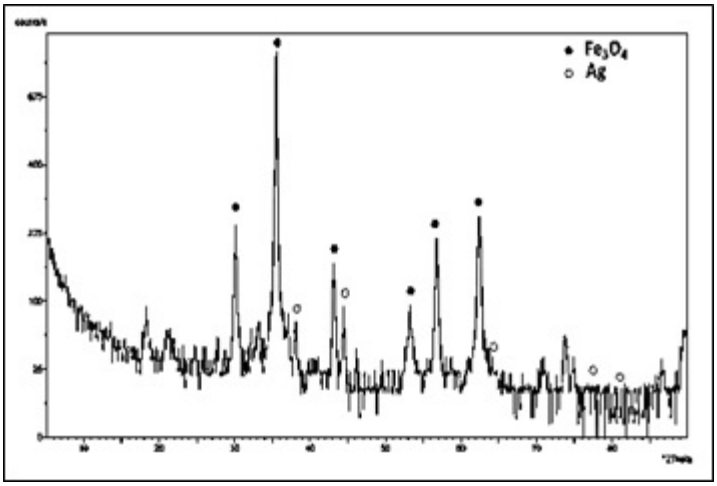

Figure 5: The XRD pattern of Fe_3O_4 NPs and Ag NPs.

4.1.3. VSM Analysis Results

The Vibrating Sample Magnetometer (VSM) analysis was conducted to determine the magnetic properties of NPs (Figure 6). Typical superparamagnetic behavior is observed for Fe_3O_4 NPs and Ag-Fe_3O_4 NPs due to the absence of any remanence or coercivity. The analysis showed the saturation magnetization (Ms) values of 61 and 69 emu/g for Fe_3O_4 NPs and Ag-Fe_3O_4 NPs, respectively. The increasing Ms. values in the nanocomposite might have been due to the interactions between the NPs that changed the anisotropic energy. There are conflicting results in the literature regarding the VSM analysis of Fe_3O_4-Ag core-shell structures. Such as, Liu et al. [39], in line with our study, reported an increase in the Ms. values when Ag was doped on the surface of Fe_3O_4 NPs, while Li et al. [40] and Ghaseminezhad and Shojaosadati [21].

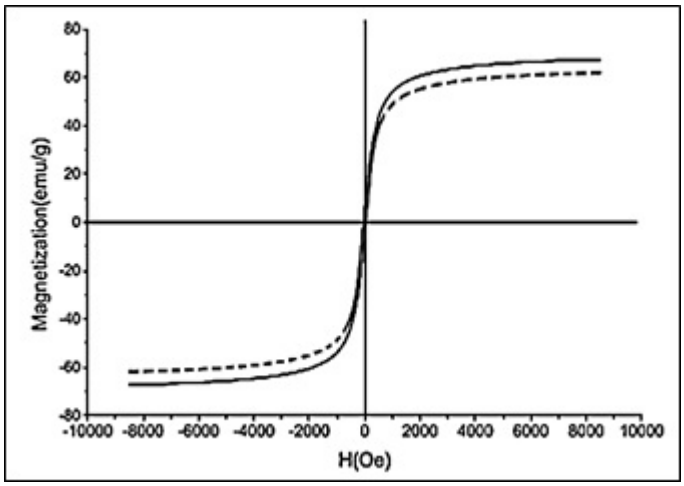

Figure 6: Magnetic hysteresis loops of Fe_3O_4 NPs (dashed line) and Ag-Fe_3O_4 NPs at 21°C.

4.2. Effect of pH on ibuprophene and oxytetracycline adsorption on Ag-Fe_3O_4 NPs

The effect of pH on the adsorption of ibuprophene and oxytetracycline on Ag-Fe_3O_4 NPs were studied within the pH ranges varying between 2.0 and 9.0. The highest degree of adsorption was achieved at pH=7.0 (Table 1).

The dependence of adsorption on pH is associated with the point of zero charge (PZC) of the Ag-Fe_3O_4 NPs and the pKa of the ibuprophene. The PZC is 6.93 for Ag. The ibuprophene is a weak acid (pKa=5.2) and exists as a neutral species por pHpKa41. For pH > 8.0 ibuprophene is deprotonated and Ag surface becomes negatively charged, thus leading to an electrostatic repulsion which reduces the adsorption efciency. For pH values greater than pKa but lower than PZC, electrostatic attraction between anionic ibuprophene and the positively charged surface of Ag NPs improves the adsorption capacity. However, the influence of initial pH of oxytetracycline adsorption on Ag-Fe_3O_4 NPs was different from the ibupprophene. When the pH was lower than 5.0, the adsorption rate increased with pH increasing. When pH was equal to 5.0, the adsorption rate reached the maximum. The maximum removal yields for ibuprophene and oxytetracycline were 99% with maximum adsorption yields of 2.03 mg/g and 3.04 mg/g for ibuprophene and oxytetracycine, respectively.

Table 1: Effect of pH on the adsorption yields of 5 mg/l ibuprophene and 5 mg/l oxytetracycline separately in the presence of 3 mg/l Ag-Fe_3O_4 NPs

pH	Ibuprophene		Oxytetracycline	
	Removal yields (%)	Adsorption (mg/g)	Removal yields (%)	Adsorption (mg/g)
4	67	0.99	56	1.34
5	68	0.99	99	3.04
6	60	0.76	54	1.03
7	99	2.03	50	0.99
8	64	0.97	43	0.76
10	40	0.56	40	0.65

4.3. Effect of Ag-Fe_3O_4 NPs concentration on the adsorptions of ibuprophene and oxytetracycline

The Ag-Fe_3O_4 NPs concentrations were increased from 0.1 mg/l up to 6.0 mg/l (Table 2). The ibuprophene and oxytetracycline concentrations were choosen as 3 mg/l at constant concentration. The volume necessary of Ag-Fe_3O_4 NPs to reach the maximum adsorption effciency is 500 µl. From 900 µl, the percentage of adsorption decreases due to the high volume of adsorbent in the medium and it is not completely removed with the magnet. 93% maximum Ag-Fe_3O_4 NPs adsorption yield was measured at 45 min contact time, 7 mg in 500 µl of suspension, at 0.1 mg/l Ag-Fe_3O_4 NPs concentration at 3.0 mg/l ibuprophene and at 3.0 mg/l oxytetracycline, respectively.

4.4. Effect of Contact time on the adsorption of Ag-Fe_3O_4 NPs to ibuprophene and oxytetracycline

The contact time between Ag-Fe_3O_4 NPs and the solution containing ibuprophene and oxytetracycline was studied from 1 to 90 min in order to achieve the maximum adsorption efficiency, reached at 45 min. From there, the percentage of adsorption remains constant until 90 min (Table 2).

The proposed method for the adsorption of ibuprophene and oxytetracycline in waters was applied to real water samples partially contaminated with this chemical compound. The concentration of the pollutant in these samples was low or not detected, so they were doped with a known concentrations of ibuprophene (3.0 mg/l) and oxytetracycline (3.0 mg/l) in order to check the viability of the proposed process. Adsorption efficiencies close to 93% were achieved in all cases, thus enabling the method as suitable for its application in real water samples (Table 2).

Table 2: Effect of Ag-Fe_3O_4 NPs concentration on the adsorption of 3.0 mg/l ibuprophene and 3.0 mg/l oxytetracycline adsorptions

Ag-Fe_3O_4 NPs concentrations (mg/l)	Ag-Fe_3O_4 NPs Adsorption (µl)	Contact Time (min)	Ag-Fe_3O_4 NPs Adsorption efficiencies (%)
0.1	500	45	93
0.5	531	43	92.7
1	580	30	91.2
1.5	612	27	90.9
2	654	24	88.6
2.5	720	10	86.5
3	735	47	83.4
3.5	756	52	71.5
4	783	65	69.8
4.5	800	77	63.4
5	841	81	55.3
5.5	876	88	51.7
6	900	90	48.9

4.5. Desorption and Recycling Studies of Ag-Fe_3O_4 NPs

The desorption of the ibuprophene and oxytetracycline from the surface of the NPs, at 1 ml HNO_3 solution, at pH=1.0 was used. For that value, interactions between adsorbent and adsorbate are weakened due to the effect of the ionic strength, as stated in the effect of pH on ibuprophene and oxytetracycline adsorption, thus favoring the desorption process. When the ibuprophene and oxytetracycline adsorptions is carried out, after separation from the aqueous solution with the magnet, this solution is decanted. Then, 1 ml HNO_3 solution is added and the mixture is sonicated for 3 min. After, the adsorbent is removed with the magnet and the acid solution is quantifed by HPLC, demonstrating that the ibuprophene and oxytetracycline total has been desorbed. Recycling studies were carried out showing that Ag-Fe_3O_4 NPs can be used during two additional successive adsorption cycles without losing adsorption capacity. In the fourth adsorption cycle, the capacity decreases down to 89.4%.

4.6. Reuse of the Ag-Fe_3O_4 Nanocomposites (NCs)

The influence of Ag-Fe_3O_4 NCs recycling on the degradation rates after one, two and three recycles under UV irradiation were 86%, 86% and 82%, respectively. And the degradation rates of one, two and three recycles under vis light irradiation were 54%, 53% and 50%, respectively. The degradation rate declined slightly with the increasing number of cycles. So Fe_3O_4-Ag NCs was effective after three recycling times.

4.7. Effect of Ag-Fe_3O_4 NPs Concentrations on the Acute Toxicity Removal Efficiencies in Pharmaceutical ww at Increasing Time and Increasing Temperature

4.7.1. Effect of Ag-Fe_3O_4 NPs Concentrations on the Microtox Acute Toxicity Removal Efficiencies in Pharmaceutical ww at Increasing Time and Increasing Temperature

The initial EC_{90} values at pH=7.0 was found as 600 mg/l at 25°C (Table 3; SET 1). After 60 min, 120 and 150 min, the EC_{90} values decreased to EC_{60}=612 mg/l to EC_{30}=429 mg/l and to EC_{10}=350 mg/l in Ag-Fe_3O_4 NPs=1 g/l at 30°C (Table 3; SET 3). The toxicity removal efficiencies were 33.33%, 66.67% and 88.89% after 60 min, 120 and 150 min, respectively, in Ag-Fe_3O_4 NPs=1 g/l at 30°C (Table 3; SET 3).

The EC_{90} values decreased to EC_{50}, to EC_{20} and to EC_5 after 60 min, 120 and 150 min, respectively, in Ag-Fe_3O_4 NPs =1 g/l at 60°C (Table 3; SET 3). The EC_{50}, the EC_{20} and the EC_5 values were measured as 607 mg/l, 482 and 357 mg/l, respectively, in Ag-Fe_3O_4 NPs =1 g/l at 60°C. The toxicity removal efficiencies were 44.44%, 77.78% and 94.44% after 60 min, 120 and 150 min, respectively, in Ag-Fe_3O_4 NPs=1 g/l at 60°C. 94.44% maximum Microtox acute toxicity yield was observed in Ag-Fe_3O_4 NPs=1 g/l after 150 min, at 60°C (Table 3; SET 3).

The EC_{90} values decreased to EC_{60}=614 mg/l to EC_{35}=498 and to EC_{15}=354 mg/l after 60 min, 120 and 150 min, respectively, in Ag-Fe_3O_4 NPs =0.5 g/l at 30°C (Table 3; SET 3). The EC_{90} values decreased to EC_{65}=603 mg/l to EC_{40}=448 and to EC_{25}=327 mg/l after 60 min, 120 and 150 min, respectively, in Ag-Fe_3O_4 NPs=1.5 g/l at 30°C. The toxicity removal efficiencies were 83.33% and 72.22% in 0.50 and 1.5 g/l Ag-Fe_3O_4 NPs, respectively, after 150 min at 30°C. It was observed an inhibition effect of Ag-Fe_3O_4 NPs=1.5 g/l to *Vibrio Fischeri* microorganisms after 150 min at 30°C (Table 3; SET 3).

The EC_{90} values decreased to EC_{60}=605 mg/l to EC_{30}=494 and to EC_{10}=454 mg/l after 60 min, 120 and 150 min, respectively, in Ag-Fe_3O_4 NPs =0.5 g/l at 60°C (Table 3; SET 3). The EC_{90} values decreased to EC_{60}=696 mg/l to EC_{35}=579 and to EC_{20}=452 mg/l after 60 min, 120 and 150 min, respectively, in Ag-Fe_3O_4 NPs =1.5 g/l at 60°C. The toxicity removal efficiencies were 88.89% and 77.78% in 0.5 and 1.5 g/l Ag-Fe_3O_4 NPs, respectively, after 150 min, at 60°C. It was observed an inhibition effect of Ag-Fe_3O_4 NPs=1.5 g/l to *Vibrio Fischeri* microorganisms after 150 min at 60°C (Table 3; SET 3).

Table 3: Effect of increasing Ag-Fe_3O_4 NPs concentrations on Microtox acute toxicity in Pharmaceutical ww at 30°C and at 60°C.

No	Parameters	Microtox Acute Toxicity Values, * EC (mg/l)							
		25°C							
		0. min		60. min		120. min		150. min	
		*EC_{90}		*EC		*EC		*EC	
1	Raw ww, control	600		EC_{80}=610		EC_{60}=510		EC_{50}=525	
		30°C				60°C			
		0 min	60. min	120 min	150. min	0 min	60. min	120. min	150. min
		*EC_{90}	*EC	*EC	*EC	*EC_{90}	*EC	*EC	*EC
2	Raw ww, control	600	EC_{70}= 610	EC_{50}= 590	EC_{40}= 680	600	EC_{60}= 680	EC_{40}= 610	EC_{30}= 410
3	Ag-Fe_3O_4 NPs=0.5 g/l	600	EC_{60}= 614	EC_{35}= 498	EC_{15}= 354	600	EC_{60}= 605	EC_{30}= 494	EC_{10}= 454
	Ag-Fe_3O_4 NPs=1 g/l	600	EC_{60}= 612	EC_{30}= 429	EC_{10}= 350	600	EC_{50}= 607	EC_{20}= 482	EC_5= 357
	Ag-Fe_3O_4 NPs=1.5 g/l	600	EC_{65}= 603	EC_{40}= 448	EC_{25}= 327	600	EC_{60}= 696	EC_{35}= 579	EC_{20}= 452

* EC values were calculated based on COD_{dis} (mg/l).

4.7.2. Effect of Ag-Fe_3O_4 NPs Concentrations on the *Daphnia magna* Acute Toxicity Removal Efficiencies in Pharmaceutical ww at Increasing Time and Increasing Temperature

As seen in Table 4; SET 1, the initial EC_{50} values were observed as 618 mg/l at 25°C. After 60 min, 120 and 150 min, the EC_{50} values decreased to EC_{35}=325 mg/l to EC_{20}=170 mg/l and to EC_{10}=70 mg/l in Ag-Fe_3O_4 NPs=1 g/l at 30°C (Table 4; SET 3). The toxicity removal efficiencies were 30%, 60% and 80% after 60 min, 120 and 150 min, respectively, in Ag-Fe_3O_4 NPs=1.00 g/l at 30°C (Table 4; SET 3).

The EC_{50} values decreased to EC_{30}=360 mg/l to EC_{15}=140 mg/l and to EC_5=39 mg/l after 60 min, 120 and 150 min, respectively, in Ag-Fe_3O_4 NPs=1 g/l at 60°C (Table 4; SET 3). The toxicity removal efficiencies were 40%, 70% and 90% after 60 min, 120 and 150 min, respectively, in Ag-Fe_3O_4 NPs=1 g/l at 60°C. 90% maximum *Daphnia magna* acute toxicity yield was observed in Ag-Fe_3O_4 NPs=1 g/l after 150 min, at 60°C (Table 4; SET 3).

The EC_{50} values decreased to EC_{40}=485 mg/l to EC_{25}=370 and to EC_{15}=190 mg/l after 60 min, 120 and 150 min, respectively, in Ag-Fe_3O_4 NPs=0.5 g/l at 30°C (Table 4; SET 3). The EC_{50} values decreased to EC_{45}=330 mg/l to EC_{30}=170 and to EC_{20}=6.50 mg/l after 60 min, 120 and 150 min, respectively, in Ag-Fe_3O_4 NPs=1.5 g/l at 30°C. The *Daphnia magna* acute toxicity yields were 70% and 60% in 0.5 and 1.5 g/l Ag-Fe_3O_4 NPs, respectively, after 150 min, at 30°C. It was observed an inhibition effect of Ag-Fe_3O_4 NPs=1.5 g/l to *Daphnia magna* after 150 min, at 30°C (Table 4; SET 3).

The EC_{50} values decreased to EC_{35}=375 mg/l to EC_{20}=23 and to EC_{10}=135 mg/l after 60 min, 120 and 150 min, respectively, in

Ag-Fe_3O_4 NPs=0.5 g/l at 60°C (Table 4; SET 3). The EC_{50} values decreased to EC_{40}=400 mg/l to EC_{25}=125 and to EC_{15}=33 mg/l after 60 min, 120 and 150 min, respectively, in Ag-Fe_3O_4 NPs=1.5 g/l at 60°C. The Microtox acute toxicity yields were 80% and 70% in 0.5 and 1.5 g/l Ag-Fe_3O_4 NPs, respectively, after 150 min, at 60°C. It was obtained an inhibition effect of Ag-Fe_3O_4 NPs=1.5 g/l to *Daphnia magna* after 150 min, at 60°C (Table 4; SET 3).

The maximum *Daphnia magna* acute toxicity removal was 90% at the Ag-Fe_3O_4 NPs concentration of 1 g/l at 60°C after 150 min (Table 4; SET 3). In this acute toxicity reduction the EC_{50} value of raw Pharmaceutical ww decreased to EC_5=39 mg/l. Low acute toxicity removals found at high Ag-Fe_3O_4 NPs concentrations could be attributed to their detrimental effect on the *Daphnia magna* cells. High Ag-Fe_3O_4 NPs (> 1.5 g/l) caused lysis in *Daphnia magna* cells. The high salt concentrations caused turgor in *Daphnia magna* cells by increasing the osmotic pressure in the test medium.

A strong significant correlation between EC_{50} values and the removal of microorganisms and organic compounds from Pharmaceutical ww showed that the *Daphnia magna* acute toxicity test alone can be considered a reliable indicator of Pharmaceutical ww toxicity (R^2=0.86, F=4.78, p=0.001). Similarly, a strong linear correlation between threshold concentrations of Ag-Fe_3O_4 NPs decrease in inhibitions was observed (R^2=0.87, F=16.72, p=0.001) while the correlation between the inhibition decrease and Ag-Fe_3O_4 NPs concentrations above the threshold values was weak and not significant (R^2=0.31, F=3.42, p=0.001).

The toxicity of Pharmaceutical ww samples to the tested species prior and after Ag-Fe_3O_4 NPs concentrations. The raw Pharmaceutical ww samples induced 95% motility inhibition to *D. magna* (Table 4; SET 3). This inhibition could be attributed to the mixed recalcitrant carcinogenic Pharmaceutical ww with high benzene rings and to the synergistic effects of the aforementioned more hydrophobic organic compounds with less hydrophobic organic compunds in Pharmaceutical ww. When *D. magnas* were exposed to the effluent Pharmaceutical ww samples after Ag-Fe_3O_4 NPs concentrations of there was a significant reduction in inhibition (from 98.90% to 99.99%) for the acute toxicity after 150 min, at 60°C (Table 4; SET 3).

Low acute toxicity removals found at high Ag-Fe_3O_4 NPs concentrations could be attributed to their detrimental effect on the *D. magna* cells. High Ag-Fe_3O_4 NPs caused lysis in *D. magna* cells. The high salt concentrations caused plasmolysis in *D. magna* cells by increasing the osmotic pressure in the test medium.

Table 4: Effect of increasing Ag-Fe_3O_4 NPs concentrations on *Daphnia magna* acute toxicity in Pharmaceutical ww at 30°C and at 60°C.

No	Parameters	***Daphnia magna* Acute Toxicity Values, * EC (mg/l)**							
		25°C							
		0. min	**60. min**			**120. min**		**150. min**	
		***EC_{50}**	***EC**			***EC**		***EC**	
1	Raw ww, control	618	EC_{45}=425			EC_{40}=325		EC_{35}=182	
		30°C				**60°C**			
		0 min	**60. min**	**120. min**	**150. min**	**0. min**	**60 min**	**120. min**	**150. min**
		***EC_{50}**	***EC**	***EC**	***EC**	***EC_{50}**	***EC**	***EC**	***EC**
2	Raw ww, control	618	EC_{40}= 510	EC_{35}= 340	EC_{30}= 85	618	EC_{40}= 425	EC_{30}= 190	EC_{25}= 32
3	Ag-Fe_3O_4 NPs=0.5 g/l	618	EC_{40}= 485	EC_{25}= 370	EC_{15}= 190	618	EC_{35}= 375	EC_{20}= 23	EC_{10}= 135
	Ag-Fe_3O_4 NPs=1 g/l	618	EC_{35}= 325	EC_{20}= 170	EC_{10}= 70	618	EC_{30}= 360	EC_{15}= 140	EC_5= 39
	Ag-Fe_3O_4 NPs=1.5 g/l	618	EC_{45}= 330	EC_{30}= 170	EC_{20}= 6.5	618	EC_{40}= 400	EC_{25}= 125	EC_{15}= 33

* EC values were calculated based on COD (mg/l).

4.7.3. Direct Effects of Ag-Fe_3O_4 NPs Concentrations on the Acute Toxicity of Microtox and *Daphnia magna* in Pharmaceutical ww

The acute toxicity test was performed in the samples containing 0.5 g/l, 1 and 1.5 g/l Ag-Fe_3O_4 NPs concentrations. In order to detect the direct responses of Microtox and *Daphnia magna* to the increasing Ag-Fe_3O_4 NPs concentrations the toxicity test were performed without Pharmaceutical ww. The initial EC values and the the EC_{50} values were measured in the samples containing increasing Ag-Fe_3O_4 NPs concentrations after 150 min. Table 5 showed the responses of Microtox and *Daphnia magna* to increasing Ag-Fe_3O_4 NPs concentrations.

The acute toxicity originating only from 0.5 g/l, 1 and 1.5 g/l Ag-Fe_3O_4 NPs concentrations were found to be low (Table 5). 0.5 g/l Ag-Fe_3O_4 NPs did not exhibited toxicity to *Vibrio Fischeri* and *Daphnia magna* before and after 150 min. The toxicity atributed to the 1 g/l and 1.5 g/l Ag-Fe_3O_4 NPs concentrations were found to be low in the samples without Pharmaceutical ww for the test organisms mentioned above. The acute toxicity originated from the Ag-Fe_3O_4 NPs decreased significantly to EC_1 and EC_4 after 150 min. Therefore it can be concluded that the toxicity originating from the Ag-Fe_3O_4 NPs is not significant and the real acute toxicity throughout the removal of microorganisms and organic compounds was attributed to the Pharmaceutical ww, to the microorganisms and organic compounds in Pharmaceutical ww ww, to their metabolites and to the disruption by-products (Table 5).

Table 5: The responses of Microtox and *Daphnia magna* acute toxicity tests in addition of increasing Ag-Fe_3O_4 NPs concentrations without Pharmaceutical ww ww after 150 min.

Ag-Fe_3O_4 NPs Conc. (g/l)	Microtox Test			*Daphnia magna* Test		
	Initial Acute Toxicity EC_{50} Value (mg/l)	Inhibitions after 150 min	EC Values (mg/l)	Initial Acute Toxicity EC_{50} Value (mg/l)	Inhibitions after 150 min	EC Values (mg/l)
0.5	EC_{10}=25	-	-	EC_{10}=30	-	-
1	EC_{15}=130	2	EC_1=5.00	EC_{20}=150	5	EC_3=8.00
1.5	EC_{20}=210	5	EC_4=10.00	EC_{30}=250	7	EC_7=12.00

5. Conclusions

This present study, the proposes a novel simple method was applied for the adsorption of ibuprophene and oxytetracycline in water using Ag-Fe_3O_4 NPs. The TEM image of Ag-Fe_3O_4 NPs appeared darker than Fe_3O_4 NPs. Our method of NPs synthesis could not produce uniform particles in size. The XRD patterns of Ag-Fe_3O_4 NPs showed the 2θ values of 38.11°, 44.32°, 64.24°, 77.61° and 81.57° corresponding to the (111), (200), (220), (311) and (222) planes of cubic Ag, respectively. The Ms values was 61 emu/g for Fe_3O_4 NPs and 69 emu/g for Ag-Fe_3O_4 NPs. The increasing Ms values in the nanocomposite might have been due to the interactions between the NPs changed the anisotropic energy.

99% maximum ibuprophene adsorption removal yield was obtained at 2.03 mg/g maximum ibuprophene adsorption concentration, at pH = 7.0 and at 21°C, respectively. 99% maximum oxytetracycline adsorption removal yield was observed at 3.04 mg/g maximum oxytetracycine adsorption concentration, at pH = 5.0 and at 21°C, respectively. 93% maximum Ag-Fe_3O_4 NPs adsorption yield was measured at 45 min contact time, 7 mg in 500 µl of suspension, at 0.1 mg/l Ag-Fe_3O_4 NPs concentration at 3.0 mg/l ibuprophene and at 3.0 mg/l oxytetracycline, respectively. The characterization of the adsorbent by means of microscopy, spectroscopy and calorimetry techniques reveal the presence of Ag in Ag-Fe_3O_4 NPs and the adsorption of ibuprophene and oxytetracycline. The adsorption equilibrium is characterized by a Langmuir isotherm model.

94.44% maximum Microtox acute toxicity yield was observed in Ag-Fe_3O_4 NPs=1 g/l after 150 min, at 60°C. However, 90% maximum *Daphnia magna* acute toxicity yield was observed in Ag-Fe_3O_4 NPs=1 g/l after 150 min, at 60°C. As a result, Microtox acute toxicity test yield is higher than *Daphnia magna* acute toxicity test for the removal of microorganisms and organic compounds from a Pharmaceutical ww using Ag-Fe_3O_4 NPs. Therefore, it can be concluded that the toxicity originating from the Ag-Fe_3O_4 NPs is not significant and the real acute toxicity throughout the removal of microorganisms and organic compounds was attributed to the Pharmaceutical ww, to the microorganisms and organic compounds in Pharmaceutical ww ww, to their metabolites and to the disruption by-products. Finaly, the removal of microorganisms and organic compounds from a Pharmaceutical ww using Ag-Fe_3O_4 NPs and the evaluation of Microtox and *Daphnia Magna* acute toxicity assays for these conditions was successfully implemented.

6. Acknowledgement

This research study was undertaken in the Environmental Microbiology Laboratories at Dokuz Eylül University Engineering Faculty Environmental Engineering Department, Izmir, Turkey. The authors would like to thank this body for providing financial support.

References

1. Najafpoor AA, Vojoudi Z, Dehgani MH, Changani F, Alidadi HA. Quality assessment of the Kashaf river in north east of Iran in 1996-2005. J Appl Sci. 2007; 7(2): 253-57.
2. Hodgson B, Sharvelle S, Silverstein JA, McKenna A. Impact of water conservation and reuse on water systems and receiving water body quality. Environ Eng Sci. 2017; 35(6): 545-59.
3. Garcia-Segura S, Ocon JD, Chong MN. Electrochemical oxidation remediation of real wastewater effluents a review. Process Saf Environ Prot. 2018; 113: 48-67.
4. Rahmani AR, Asgari G, Askari FB, Torbaghan AE. Adsorption of lead metal from aqueous solutions using activated carbon derived from scrap tires. Fresenius Environ Bull. 2015; 24(7): 2341-47.
5. Golbaz S, Nabizadeh R, Zarinkolah S, Mahvi AH, Alimohammadi M, Yousefi M. An innovative swimming pool water quality index (SPWQI) to monitor and evaluate the pools: design and compilation of computational model. Environ Monit Assess. 2019; 191(7): 448.
6. Qin L, Zeng G, Lai C, Huang D, Xu P, Zhang C, Cheng M, Liu X, Liu S, Li B, Yi H. "Gold rush" in modern science: fabrication strategies and typical advanced applications of gold nanoparticles in sensing. Coord Chem Rev. 2018; 359: 1-31.
7. Wu S, Zhang S, Gong Y, Shi L, Zhou B. Identification and quantification of titanium nanoparticles in surface water: a case study in Lake Taihu, China. J Hazard Mater. 2019; 382(5842): 121045.
8. Zhong C-J, Maye MM. Core–shell assembled nanoparticles as catalysts. Adv Mater. 2001; 13(19): 1507-11.
9. Sadegh H, Ali GAM, Gupta VK, Makhlouf ASH, Shahryari-ghoshekandi R, et al. The role of nanomaterials as effective adsorbents and their applications in wastewater treatment. J Nanostructure Chem. 2017; 7(1): 1-14.
10. Zhou X, Lai C, Huang D, Zeng G, Chen L, Qin L, et al. Preparation of water-compatible molecularly imprinted thiolfunctionalized activated titanium dioxide: selective adsorption and efficient photodegradation of 2, 4-dinitrophenol in aqueous solution. J Hazard Mater. 2018; 346: 113-23.
11. Lai C, Liu X, Qin L, Zhang C, Zeng G, Huang D, Cheng M, Xu

P, Yi H, Huang D. Chitosan-wrapped gold nanoparticles for hydrogen-bonding recognition and colorimetric determination of the antibiotic kanamycin. Mikrochim Acta. 2017; 184(7): 2097-105.

12. Shaffiey SR, Shaffiey SF. Silver oxide–copper oxide nanocomposite preparation and antimicrobial activity as a source for the treatment of fish diseases: silver oxide–copper oxide Nanocomposite preparation and antimicrobial activity. Advancing Medicine Through Nanotechnology and Nanomechanics Applications, IGI Global. 2017; 140-51.
13. Zhang X, Wang W, Zhang Y, Zeng T, Jia C, Chang L. Loading Cu-doped magnesium oxide onto surface of magnetic nanoparticles to prepare magnetic disinfectant with enhanced antibacterial activity. Colloids Surf B Biointerfaces. 2018; 161: 433-41.
14. Sponza DT, Oztekin R. Removal of microorganisms and organic compounds from a pharmaceutical wastewater using silver-loaded magnetic nanoparticles. 3rd International Webinar on Magnetism and Magnetic Materials Conference, Theme: Exploring Magnetism and Magnetic Materials with their new characteristics, Magnet. 2022.
15. Ali I, Peng C, Naz I, Khan ZM, Sultan M, Islam T, Abbasi IA. Phytogenic magnetic nanoparticles for wastewater treatment: a review. RSC Adv. 2017; 7(64): 40158-78.
16. Daraei H, Amrane A, Kamali H. Assessment of phenol removal efficiency by synthesized zero iron nanoparticles and Fe powder using the response surface methodology. Iran. J. Chem. Chem. Eng. 2017; 36(3): 137-46.
17. Tran N, Mir A, Mallik D, Sinha A, Nayar S, Webster TJ. Bactericidal effect of iron oxide nanoparticles on Staphylococcus aureus. Int J Nanomedicine. 2010; 5: 277-83.
18. U.S. Public Health Service Report. Toxicological profile for silver, Agency for Toxic Substances and Disease Registry, U.S. Public Health Service, USA. 1990..
19. Fisher J, Benner S, Golden P, Edwards R. Silver toxicity: A brief overview. prepared for: Idaho Power Company, Prepared by: Boise State University and Heritage Environmental consultants. USA. 2015; 1-40.
20. https://leg.mt.gov/content/Committees/Interim/2019-2020/Water-Policy/Meetings/Jan-2020/Ag%20Toxicity%20literature%20review%20%2812-16-15%29.pdf.
21. Sachse C, Weiß N, Gaponik N, Müller-Meskamp L, Eychmüller A, Leo K. ITO-free, small-molecule organic solar cells on spray-coated coppernanowire-based transparent electrodes, Advanced Energy Materials. 2014; 4(2): 1300737.
22. Ghaseminezhad SM, Shojaosadati SA. Evaluation of the antibacterial activity of Ag/ Fe3O4 nanocomposites synthesized using starch. Carbohydr Polym. 2016; 144: 454-63.
23. Azócar MI, Alarcón R, Castillo A, Blamey JM, Walter M, Paez M. Capping of silver nanoparticles by anti-inflammatory ligands: antibacterial activity and superoxide anion generation. J Photochem Photobiol B, Biol. 2019; 193: 100-8.
24. Ghaseminezhad SM, Shojaosadati SA, Meyer RL. Ag/Fe3O4 nanocomposites penetrate and eradicate S. aureus biofilm in an in vitro chronic wound model. Colloids Surf B Biointerfaces. 2018; 163: 192-200.
25. Davoudi M, Ehrampoush MH, Vakili T, Absalan A, Asghar Ebrahimi A. Antibacterial effects of hydrogen peroxide and silver composition on selected pathogenic enterobacteriaceae. Int J Environ Health Eng. 2012; 1(1): 23.
26. Petrov DA, Ivantsov RD, Zharkov SM, Velikanov DA, Molokeev MS, Lin C-R, et al. Magnetic and magneto-optical properties of Fe3O4 nanoparticles modified with Ag. J Magn Magn Mater. 2020; 493: 165692.
27. Joshi MK, Pant HR, Kim HJ, Kim JH, Kim CS. One-pot synthesis of Ag-iron oxide/reduced graphene oxide nanocomposite via hydrothermal treatment. Colloids Surf A Physicochem Eng Asp. 2014; 446: 102-8.
28. Lange B. LUMISmini, Operating Manual. Düsseldorf, Germany: Dr Bruno LANGE. 1994.
29. Lange B. Vibrio fischeri -Microtox LCK 491 kit. Germany: Dr LANGE. 2010.
30. Lange B. LUMIXmini type luminometer. Dusseldorf: Dr LANGE Company. 1996.
31. Baird RB, Eaton AD, Rice EW. Rice EW (editors). Standard Methods for the Examination of Water and Wastewater. (23rd. Ed.). American Public Health Association (APHA), American Water Works Association (AWWA), Water Environment Federation (WEF). American Public Health Association 800 I Street, NW Washington DC: 20001-3770, USA. 2017; ISBN-13:978-0875532875; ISBN-10:087553287X.
32. Statgraphics Centurion XV, software, 2005 (Statpoint, Inc). StatPoint, Inc. Statgraphics Centurion XV. Herndon, VA. USA. 2005.
33. Wang H, Zhang W, Zhao J, Xu L, Zhou C, Chang L, Wang L. Rapid decolorization of phenolic azo dyes by immobilized laccase with Fe3O4/SiO2 nanoparticles as support. Ind Eng Chem Res. 2013; 52: 4401-7.
34. Park M, Seo S, Lee IS, Jung JH. Ultra efficient separation and sensing of mercury and methylmercury ions in drinking water by using aminonaphthalimide-functionalized Fe3O4@SiO2 core/shell magnetic nanoparticles. Chem Commun. 2010; 46: 4478 80.
35. Sun L, Li Y, Sun M, Wang H, Xu S, Zhang C, Yang Q. Porphyrin-functionalized Fe3O4@SiO2 core/shell magnetic colorimetric material for detection, adsorption and removal of Hg+2 in aqueous solution. New J Chem. 2011; 35: 2697-704.
36. Tan P, Qin J-X, Liu X-Q, Yin X-Q, Sun L-B. Fabrication of magnetically responsive core–shell adsorbents for thiophene capture: AgNO3-functionalized Fe3O4@mesoporous SiO2 microspheres. J Mater Chem A. 2014; 2: 4698-705.
37. Naqvi S, Samim M, Abdin MZ, Ahmed FJ, Maitra AN, Prashant CK, Dinda AK. Concentration-dependent toxicity of iron oxide nanoparticles mediated by increased oxidative stress. Int J Nanomedicine. 2010; 5: 983.
38. Ebrahimi N, Rasoul-Amini S, Ebrahiminezhad A, Ghasemi Y, Gholami A, Seradj H. Comparative study on characteristics and cytotoxicity of bifunctional magnetic-silver nanostructures: synthesized using three different reducing agents. Acta Metall Sin (Engl Lett). 2016; 29(4): 326-34.

39. Santoyo Salazar J, Perez L, de Abril O, Phuoc LT, Ihiawakrim D, Vazquez M, et al. Magnetic iron oxide nanoparticles in 10− 40 nm range: composition in terms of magnetite/maghemite ratio and effect on the magnetic properties. Chem. Mater. 2011; 23(6): 1379-86.

40. Liu CH, Zhou ZD, Yu X, Lv BQ, Mao JF, Xiao D. Preparation and characterization of Fe3O4/Ag composite magnetic nanoparticles. Inorg Mater. 2008; 44(3): 291-5.

41. Li W-H, Yuea X-P, Guo C-S, Lv J-P, Liu S-S, Zhang Y, Xu J. Synthesis and characterization of magnetically recyclable Ag nanoparticles immobilized on Fe3O4@ C nanospheres with catalytic activity. Appl Surf Sci. 2015; 335: 23-8.